

Detection of Meridional Currents in the Equatorial Ionosphere

G. Musmann¹ and E. Seiler²

¹ Institut für Geophysik und Meteorologie der Technischen Universität Carolo-Wilhelmina, Mendelssohnstraße 1A, 3300 Braunschweig, Federal Republic of Germany

² Physikalisch-Technische Bundesanstalt, Bundesallee 100, 3300 Braunschweig, Federal Republic of Germany

Abstract. Theoretical investigations predict meridional currents in the dynamo region of the ionosphere a few degrees north and south of the magnetic equator as a consequence of the equatorial electrojet. The magnetic fields of these currents are perpendicular to the permanent magnetic field of the earth and cause a height variation of the magnetic declination. It was the aim of six rocket launches performed in 1970 near noon at Natal, Brazil, to detect these currents. To reach this objective, identical payloads each consisting of two flux-gate magnetometers, a solar aspect sensor, an experiment to measure the angle between the magnetic field and the direction to the sun, and an impedance probe to determine the electron density were launched under different magnetic conditions. The predicted variation of the declination has been observed but with considerably higher amplitude than was expected. On the other hand, the measured height integrated current density in the west-east direction was smaller than deduced from ground based magnetic H-variations.

These discrepancies can be explained by currents flowing at 5 degrees off the magnetic equator, on both sides, with intensities of about 0.3 of the electrojet intensity at the same height but in reversed direction. Such reversed currents have recently been observed from ground based magnetic observations by others and have also been interpreted theoretically by ionospheric wind effects.

Key words: Equatorial electrojet – Meridional currents – Rocket experiments.

Introduction

Untiedt (1967) has shown that the primary eastward electric field responsible for the equatorial electrojet also gives rise to a meridional current flow perpendicular to the equator. This flow constitutes an infinite solenoid which generates a

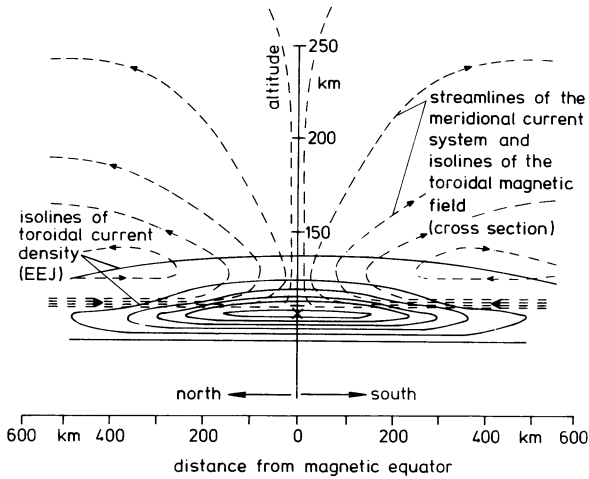


Fig. 1. Schematic drawing of the equatorial electrojet (EEJ, toroidal current system) flowing perpendicular to the plane of the figure, the meridional current system (dashed lines) and the corresponding toroidal magnetic field. Streamlines of the meridional current systems represent also isolines of the toroidal magnetic field

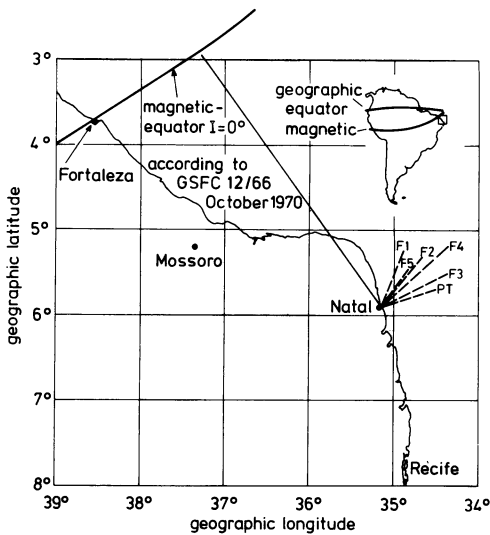


Fig. 2. Launch site Natal and horizontal projection of trajectories of the rocket flights (dashed lines). The magnetic equator is indicated. Ground based measurements of the magnetic field variations were recorded at Fortaleza, Mossoro and Natal by Askania-Variographs

toroidal east-west or west-east directed magnetic field within the ionosphere. A schematical representation of the meridional current flow and of the equatorial electrojet is shown in Figure 1.

According to calculations by Untiedt (1967), Sugiura and Poros (1969) and Richmond (1973) the two maximum absolute values of the toroidal magnetic field ΔY_M which changes sign above the magnetic equator are to be expected at about 300 to 400 km off the magnetic equator and at an altitude of about 120 km. The magnitude of these values should be about the same as that one of the magnetic variations on the ground caused by the electrojet at the magnetic equator.

Assuming a value of 160 nT for such a variation on the ground, representing a moderately developed electrojet, the toroidal magnetic field should change the

declination of the total earth's magnetic field by as much as 0.5 degrees at 120 km altitude and at the flanks of the jet. The contribution to the total field intensity at this height should be less than 1 nT because the direction of the disturbing toroidal magnetic field is nearly perpendicular to the permanent field F ($F \approx 25,000$ nT).

Because the toroidal field is confined to the ionospheric E - and F -regions it is not observable on the ground and can only be detected by means of rocket-borne vector magnetic measurements.

The present paper reports on the results of six such rocket experiments that were performed at Natal (Brazil) in October 1970. Day and time of each launch may be taken from Figure 8. Natal was selected as the launch site because it is situated about 380 km off the magnetic equator (Fig. 2), approximately below the maximum of the toroidal field strength (Fig. 1).

Description of Instrumentation

A detailed description of the instrumentation is given by Musmann (1971), therefore only some particulars of the payload will be reported on here.

On board the rocket the electron density was measured using an impedance probe developed by Melzner and Rabben (1970). The components of the magnetic field parallel and perpendicular to the spin axis of the rocket were determined by flux gate magnetometers (Förstersonde). The spin modulations of the magnetometer outputs were eliminated on board by filtering. It was therefore possible to limit the measuring range for the component R perpendicular to the spin axis to 8,000 nT with a constant offset of 20,000 nT while the measurement range of the longitudinal component L was 0 to 13,000 nT. Using a fast 12 bit A/D -converter a resolution of about ± 1 nT for the radial (R) and ± 1.5 nT for the longitudinal component (L) was obtained.

The sampling rate for all sensors was triggered by a precision differential sun slit sensor giving one pulse per rotation of the rocket. For each rotation (spin frequency approximately 10 Hz) the field magnitude F and the angle α between the figure axis of the rocket and the field vector were calculated according to $F = (R^2 + L^2)^{1/2}$ or $\tan \alpha = R/L$ respectively. The resolution of α is about one minute of arc.

The angle ψ between sun direction and figure axis (see Fig. 3) was measured with a high accuracy solar aspect sensor developed by Ernst Leitz GmbH, Optische Werke, Wetzlar, Germany. The resolution of this sensor was 1.8 min of arc.

From the rocket data the variation of declination is seen in the variation of the azimuth angle ν between the sun meridian indicated by the sun slit sensor and the direction of the magnetic field detected by a search coil. This angle ν was determined as the time difference between both signals. The time resolution was 1 μ s corresponding to a resolution of 0.4 min of arc.

In addition the spin period of the rocket was measured with the same precision slit sensor with a resolution of 4 μ s. Four payloads operated successfully ($F1$, $F3$, $F4$, and PT). One failed partially, and for one flight the solar aspect sensor was out of range.

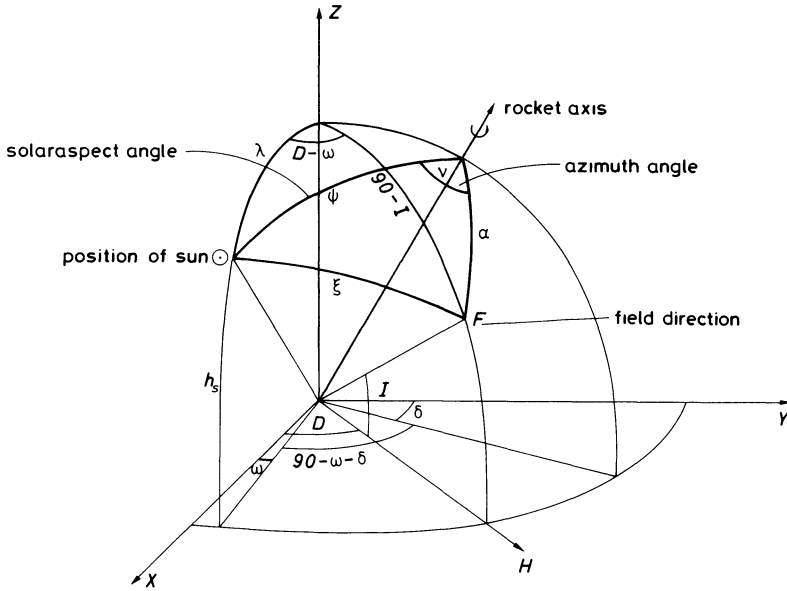


Fig. 3. Coordinate system defining the measured angles α, ψ, ν . x, y geographical north and west direction; D, I, H magnetic declination, inclination, and horizontal component, respectively

Identification of the Toroidal Field

In Figure 3 the sun is represented by its coordinates λ (distance from zenith) and ω (azimuth). These values can be calculated for each flight using the geographical coordinates of Natal, the launch time, data from the Nautical Yearbook 1970, and the tracked trajectory of the rocket. The flight altitude of the rocket is negligible when compared to the distance of the sun. The direction of the magnetic field vector \mathbf{F} is characterized by the inclination I and the declination D .

The spherical triangle given by the direction towards the sun, the field vector \mathbf{F} and the rocket figure axis (Fig. 3), is determined by the measured solar aspect angle ψ , the field direction angle α , and the azimuthal angle ν . From these measured quantities the angle ξ between sun and magnetic field direction, here named ξ_1 can be calculated according to the equation

$$\cos \xi_1 = \cos \psi \cos \alpha + \sin \psi \sin \alpha \cos \nu \tag{1}$$

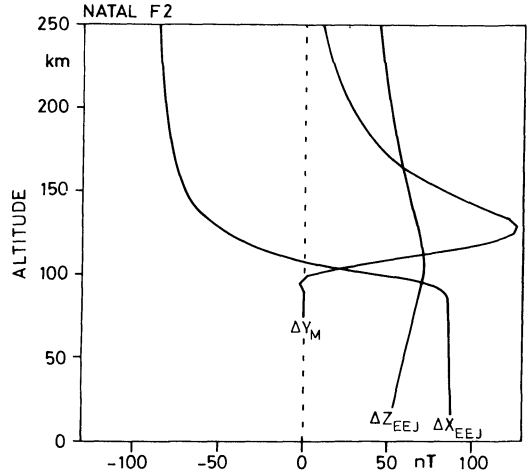
with an error of a few minutes of arc.

The orientation of the spherical triangle in space is not considered because it is of no interest for the subject in question. ξ_1 is the "measured value" of ξ .

On the other hand a second value for ξ (named ξ_2) can be calculated using the triangle represented by the sun's direction, the field vector \mathbf{F} , and the vertical axis Z , from calculated values of λ, ω, I , and D :

$$\cos \xi_2 = \cos \lambda \sin I + \sin \lambda \cos I \cos (D - \omega) \tag{2}$$

Fig. 4. Vertical (ΔZ_{EEJ}) and northward (ΔX_{EEJ}) components of magnetic variation produced by the equatorial electrojet as function of height at Natal. ΔY_M is the magnetic variation in east direction expected from the meridional currents. Calculations by Rippen (1975) according to Untiedt's (1967) model for rocket experiment F2 conditions



I and D , respectively, are the undisturbed values for inclination and declination of the earth's magnetic field along the trajectories. The variations of the inclination and declination produced by the main electrojet without meridional currents can be neglected. Therefore ξ_2 is a "calculated value" of ξ , neglecting the influence of the meridional currents.

Figure 4 shows the predicted variations with height of the field components ΔX_{EEJ} , ΔZ_{EEJ} , and ΔY_M as produced by the main electrojet (index EEJ) and by the meridional current system (index M), respectively.

It is assumed that the difference between the measured and the calculated values ξ , namely between ξ_1 and ξ_2 , must be caused by the meridional current system via ΔD_M , the variation in declination caused by the meridional current system. According to Untiedt's (1967) model significant values of ΔD_M are to be expected in the region $90 \text{ km} \leq h \leq 130 \text{ km}$ only. Therefore ξ_1 and ξ_2 should be identical with the exception of this region where the meridional currents are flowing.

However there can be a systematic deviation between the two curves $\xi_1(h)$ and $\xi_2(h)$ due to differences between the actual values of D and I and those calculated from spherical harmonic expansions, which are used to determine $\xi_2(h)$. However, this difference is not critical as will be shown later. If the influence of the meridional current system (ΔD_M) is taken into account, $D - \omega$ has to be replaced by $D - \omega + \Delta D_M$ in Equation (2), and also ξ_2 has to be replaced by ξ_1 . This yields the relation

$$\begin{aligned} \cos \xi_1 = & \cos \lambda \sin I + \sin \lambda \cos I \cos(D - \omega) \cos \Delta D_M \\ & - \sin \lambda \cos I \sin(D - \omega) \sin \Delta D_M. \end{aligned} \quad (3)$$

ΔD_M is expected to be $< 1^\circ$, that means $\cos \Delta D_M \geq 0.9998$. Therefore we use $\cos \Delta D_M = 1$. ΔI_M is assumed to be zero because the meridional currents produce no vertical magnetic disturbance.

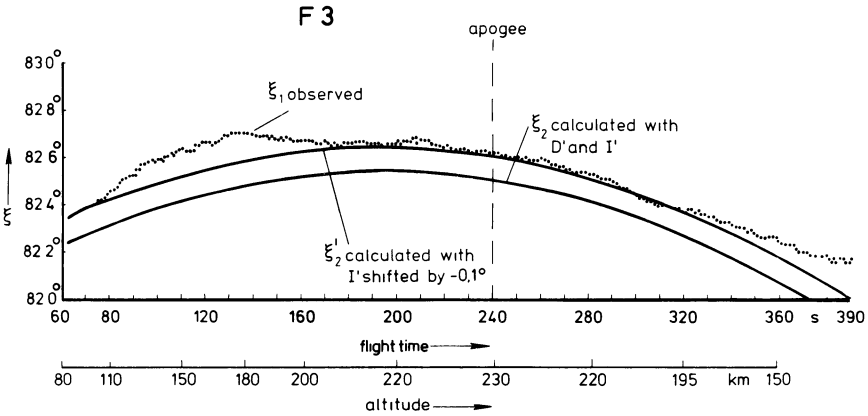


Fig. 5. Example (experiment *F 3*) of observations of ξ_1 and calculations of ξ_2 as function of flight time. For exact definition of the angles (cf. Fig. 3) ξ_1 and ξ_2 see text. ξ_2' shows the influence of a constant shift in inclination I by -0.1° which gives the best approximation to ξ_1 in the regions where the influence of the meridional current systems should be negligible

Now, the combination of Equations (2) and (3) yields

$$\sin \Delta D_M = \frac{\cos \xi_2 - \cos \xi_1}{\sin \lambda \cos I \sin (D - \omega)} \tag{4}$$

The values of D and I can be calculated according to Cain et al. (1968) using the spherical harmonic expansion of the earth's magnetic field and the NASA GSFC 12/66 set of coefficients with deviations (actual main magnetic field minus computed field) of about $\pm 0.2^\circ$ for the flight area.

Due to the uncertainties in the spherical harmonic expansion a small but nearly constant deviation between $\xi_1(t)$ and $\xi_2(t)$ may be expected. This deviation may be eliminated by including a constant shift of D and I in the calculation of $\xi_2(t)$. Figure 5 shows the effect of such a shift in I (as an example). Apparently, only by including such a constant shift it is possible to match ξ_1 and ξ_2 below and above the height region of meridional currents. The finally adopted shift of $I - 0.1^\circ$ represents the best fit between ξ_1 and ξ_2 for $h < 90$ km and $h > 200$ km. For all flights the curves $\xi_2(t)$ were adjusted in the same manner.

Observational Results

All impedance probe measurements show a fairly smooth increase of the electron density with height and are similar in character. Therefore only the results of flight *F 5* are shown in Figure 6 as an example. More details about these measurements are given by Mühlhausen (1974). The results also agree with other observations of electron densities in the equatorial ionosphere, e.g. (Aikin and Blumle, 1968), (Jacobs and Rawer, 1966), (Jacobs and Rawer, 1965), and (Maynard, 1967).

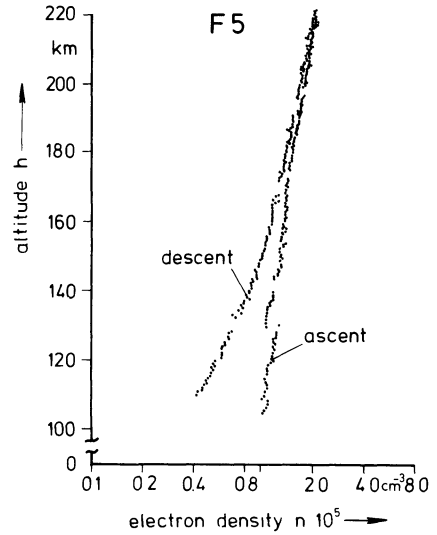


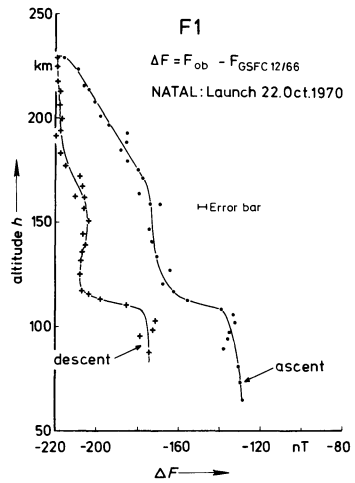
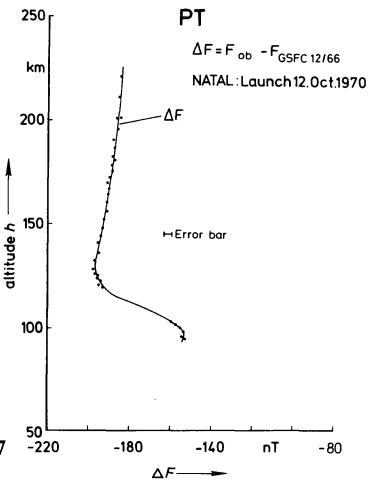
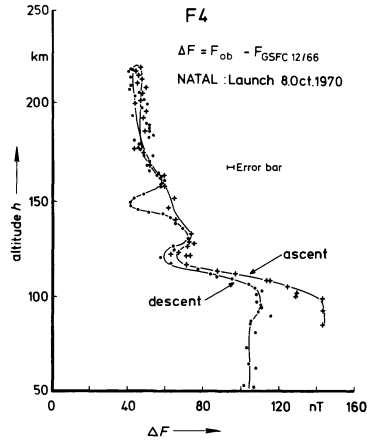
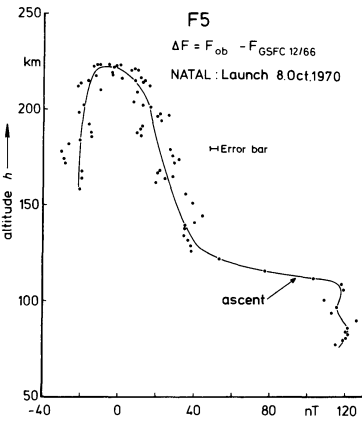
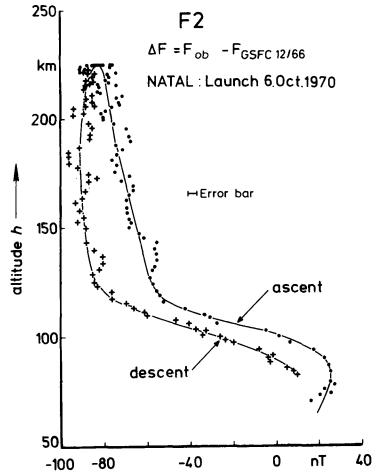
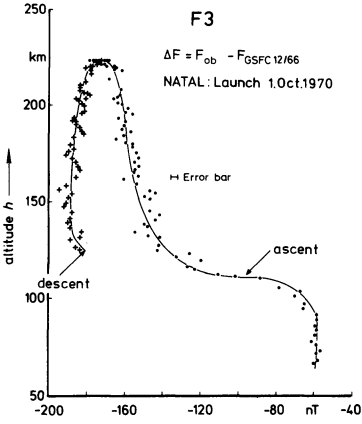
Fig. 6. Observed electron density profile for flight *F 5*

From the two magnetometer outputs R and L the field magnitude F_{ob} was calculated according to $F_{ob} = (R^2 + L^2)^{1/2}$. A field magnitude F_{GSFC} computed according to Cain et al. (1968) using the NASA GSFC 12/66 set of coefficients was subtracted from the observed field F_{ob} to get the observed field intensity difference ΔF . These values of ΔF are shown as a function of height in Figure 7 for the different rocket experiments. Only differences of ΔF are meaningful, because no zero adjustment has been made in all these cases. The remarkably nearly parallel shifts in ascent and descent curves for flights F_1 , F_3 , and F_5 are mainly due to uncertainties in the determination of the rocket trajectories. This is due to the fact that only skin tracking radar observations for limited time intervals after launch were available.

During all the flights a steep decrease in ΔF is to be seen beginning at altitudes of 100 km for flights, F_3 , F_4 , and PT , at about 110 km for F_1 and F_5 , and at 90 km for F_2 . A second but not as well defined change in slope is to be seen at 125 km for F_2 , F_4 , PT , at 130 km for F_3 , and F_5 , and at 120 km for F_1 . If we assume that the observed slope is due to the main electrojet current a variation in thickness of the current layer from about 15 to 35 km may be derived.

A close correlation between the magnitude of the magnetic variation in the horizontal component H on the ground and the total variation of ΔF with height is to be expected. Figure 8 shows the H traces as observed at Natal for all six rocket launches, taken from Musmann et al. (1971). If we define ΔH as the difference between the H component during rocket flight and the H level of the two nights before and afterwards, it may be seen (Table 1) that ΔH is nearly equal to ΔF_{total} . On the other hand, the relation $\Delta F_{total} \approx 2 \cdot \Delta H$ when passing the current layer should hold, if the internal part within ΔH is being neglected. A possible explanation for this apparent discrepancy will be given below.

During the flights F_1 and F_4 some special features are to be seen in the ΔF



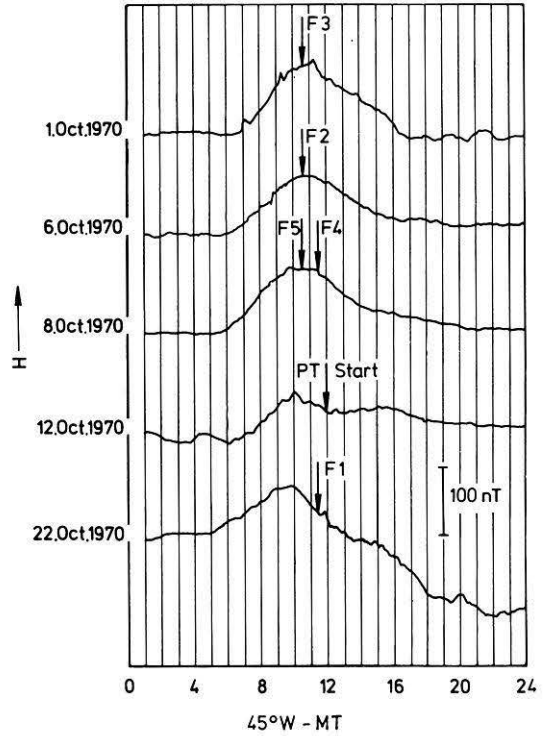


Fig. 8. Horizontal magnetic field variations H observed on the ground at Natal during launch days. Actual launch times are marked by arrows

Table 1. The measured total ΔF variation during flight and the ground observation of ΔH at Natal for the flight time

	ΔF (flight)		ΔH Natal
	ascent (nT)	descent (nT)	ground (nT)
F 1	45	45	≈ 30 (disturbed)
F 2	80	80	80
F 3	100		100
F 4	100	60	88 (decreasing to 80)
F 5	100		92
PT	40		≈ 30 (disturbed)

Fig. 7. Differences ΔF between observed (F_{ob}) and calculated (F_{GSFC}) field magnitudes versus altitude, for the different rocket experiments. Only every tenth measured value has been plotted. Differences between ascent and descent are due to uncertainties in trajectory determination and in spherical harmonic representation of the actual permanent magnetic field. The abscissa values are not corrected for absolute numbers, because only the variations of magnitude are of interest. The small periodical variations in the representations for F 2, F 3 and F 5 are due to the influence of the on board spin demodulation on the nutation modulation of the magnetometer outputs

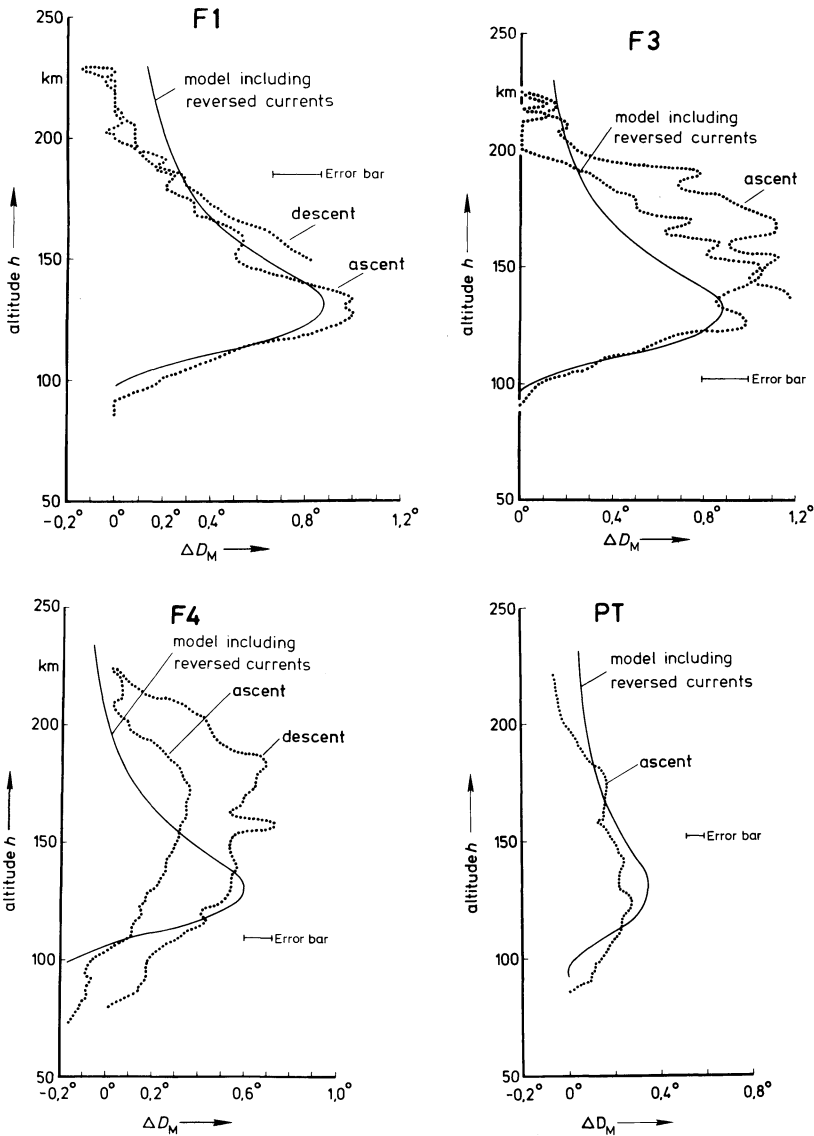


Fig. 9. The existence of meridional currents is seen in the measured variation ΔD_M of the declination with altitude. Each point of the dotted lines represents an average of 10 measured values. The solid lines represent model calculations including currents on both sides of the equator with intensities of 0.3 of the electrojet but in reversed direction

curves: For flight *F1* a change in ΔF occurred when the ground observations showed a small positive change in the decreasing phase of H indicating also a temporary increase of the current density. The ΔF curve for flight *F4* showed two significant extreme values at about 150 km and 125 km during the descent. These variations were not seen in the ground data, which only showed a steep

Table 2.

Flight	Max. value of ΔD_M degrees	ΔH (magn. Equator) (nT)	ΔY_M (nT)	ΔH_E (nT)
<i>F 1</i>	≈ 1	(disturbed)	≈ 430	?
<i>F 3</i>	≈ 1	185	≈ 430	346
<i>F 4</i>	0.7	170	300	284
<i>PT</i>	0.3	80	130	121

decrease in H of nearly 10 nT during the flight time. Therefore the variations during this flight must be due to locally enhanced current densities.

While the effect of the electrojet is seen in ΔF , the disturbance of the meridional current is observed as a variation ΔD_M of the declination D . To get this variation ξ_1 was calculated according to Equation (1). This was possible for the four successful flights *F 1*, *F 3*, *F 4*, and *PT*. The computed curves of ξ_2 were shifted as discussed above in connection with Figure 5 to get a good agreement between the curves $\xi_1(h)$ and $\xi_2(h)$ above 200 km as expected although the corrections are only made for $h \leq 90$ km altitude. A deviation between both curves can clearly be seen in Figure 5, as an example, between 100 km and 200 km altitude. This deviation is considered to be due to the effect of the meridional currents of the electrojet system.

To get ΔD_M Equation (4) is used. The term $(\sin \lambda \cos I \sin(D - \omega))^{-1}$ is of the order of 7 to 10 for all flights and varies only slightly during a special flight. It can be determined with a possible error of $\pm 10\%$. The ΔD_M results for the four flights are shown in Figure 9. Each point of the dotted lines in Figure 9 represents an average of 10 measured values. As expected from the electrojet model the maxima of ΔD_M occur at higher levels than the main electrojet and are much broader.

The measured maximum values of ΔD_M are given in Table 2 for the four flights, together with the instantaneous values of ΔH at the magnetic equator (station Fortaleza) and values of ΔY_M which is the toroidal field strength from the given ΔD_M . The meaning of ΔH_E will be explained later.

Although there seems to exist some correlation between ΔH and ΔY_M within Table 2 the observed $\Delta Y_M/\Delta H$ amounting to about 2 is larger than has to be expected from Untiedt's (1967) model. According to this model the ΔY_M maximum value should be comparable to the equatorial ΔH variation at the ground.

Possible Explanation of the Observations

Although the equatorial electrojet and the toroidal magnetic fields of the predicted meridional currents have been observed within our rocket experiments there seem to exist two discrepancies:

1. The measured total ΔF variation with height is considerably smaller than expected from the ground ΔH measurements via calculations according to Untiedt's (1967) model.

2. The observed toroidal magnetic field ΔY_M is larger than predicted by Untiedt's (1967) model by about a factor of 2.

In addition to recent results from ground based magnetic observations (Fambitakoye and Mayaud, 1976a and b; Hesse, 1977, private communication) our results indicate that the influence of other currents has to be taken into account.

The ground based observations mentioned clearly have shown the existence of two secondary current ribbons flowing at about 500 km distance from the magnetic equator in a direction which is opposite to the direction of the main electrojet. Richmond (1973) has shown that an electrojet model including the effects of height-dependent ionospheric east-west winds is able to generate such secondary current ribbons. His model has been applied by Fambitakoye et al. (1976c) to explain the recent observations of Fambitakoye and Mayaud (1976a and b). Accordingly, we assume that the observed magnetic variations ΔH on the ground are a superposition of the effects of the following currents: the equatorial electrojet, the reversed currents north and south of the equator, the normal Sq-current system, and their induced currents.

For each rocket flight the ΔH variation on ground was measured at the three stations Fortaleza ($d=0$ km, d =distance from the magnetic equator), Mossoro ($d=180$ km) and Natal ($d=370$ km) [Musmann et al., 1971].

For the simplified model three equivalent line currents were selected: a line current at an altitude of 500 km above the magnetic equator and two reversed line currents at an altitude of 400 km at a distance of 500 km north and south from the magnetic equator with 0.3 the current intensity of the main electrojet. These equivalent line currents representing the main electrojet and the reversed currents, respectively, are producing the same magnetic variations on the ground as the measured quantities. The heights and distances of the line currents from the magnetic equator were selected to match the observed latitudinal field distribution on ground while the ratio of the current densities was chosen to give a best fit to the H -observations at Natal and Fortaleza.

For adaptation of the model there are still three variables free: The current intensity I of the electrojet line current, a part of ΔH which is independent of d (representing the contribution from the Sq current system) and the depth T of an infinitely conductive layer for modelling the induced currents.

A value of $T=200$ km was selected which gives maximum influence of the induced currents, according to observations reported by Sastry (1973), Davis et al. (1967), and Hesse (1977, private communication). On the other hand, Fambitakoye and Mayaud (1976a) have shown that the effective depth for image earth currents must be greater than 1200 km for regular variations. Therefore in Figure 10 also the $\Delta H(d)$ profile including no effects from induced currents, i.e. for the case $T=\infty$, are shown to demonstrate all possible values between maximum and zero influence. To $\Delta H(d)$ in Figure 10 one possible profile of Sq as observed in Brazil (Hesse, private communication) was added. The absolute value of the electrojet current intensity I was selected to match the observations of ΔH in Natal. Using this simplified model it is possible to calculate the influence in the observed H values of the reversed currents for the station Fortaleza (magnetic equator). In Table 2 the value ΔH_E is representing this corrected ΔH value.

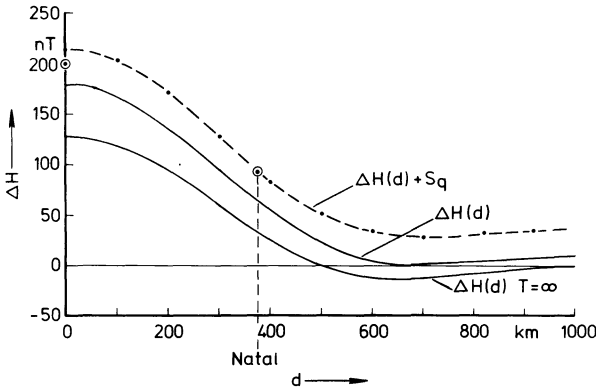


Fig. 10. Model calculations for $\Delta H(d)$ on the ground for the electrojet and two reversed currents at a distance of $d=500$ km north and south of the equator with a current intensity of 0.35 each with respect to the electrojet. The induced currents assuming a perfect conductor at a depth of $T=200$ km are included in the curves of $\Delta H(d)$ and $\Delta H(d)+S_q$. One possible S_q profile taken from ground based observations (Hesse, private communication) is added to $H(d)$ to get $\Delta H(d)+S_q$. (S_q is about 30 nT for Natal). For comparison a profile neglecting induced currents ($T=\infty$) is also shown. The magnitude of the electrojet current was chosen to get the best agreement at $d=0$ km (Fortaleza) and $d=370$ km (Natal) with ground observations for flight *F 3*. The observations of H on the ground at Fortaleza and Natal are marked (\otimes)

According to Untiedt’s model this value ΔH_E would be comparable with the maximum value of ΔY_M of the toroidal field. As can be seen in Table 2 this is now in good agreement so that the second discrepancy cited above has been removed. In Figure 9 the solid lines represent calculations of $\Delta D(h)$ including the influence of reversed currents of 0.3 the strength of the electrojet. The agreement with observations is fairly good for *F 1* and *PT*, whereas the results for *F 3* and *F 4* differ significantly in the shapes of the curves but not so much in amplitudes. This may be due to meridional currents with other current distributions.

In order to predict $\Delta F(h)$ the variation with height for Natal ($d=370$ km) from this simple model, an equivalent current density $J(d)$ at 100 km height has been calculated under the condition that it produces the same magnetic field as the three line currents mentioned above between this height and the ground. For heights greater than 100 km the magnetic field is assumed to be that of the current layer $J(d)$ with zero thickness. Therefore there is a jump in $\Delta H(h)$ at 100 km. If one includes also the field of the induced currents, one obtains $\Delta H(h)$ profiles for any distance d which can be compared with the measured flight profile, approximately.

Figure 11 shows the calculated profile $\Delta H(h)$ for $d=0$ (magnetic equator) and $d=370$ km (Natal). The asymmetry with respect to the line $\Delta H = \Delta F = 0$ nT results from the fact that the magnetic field of the induced currents does not change sign at the height of the electrojet. In addition to the theoretical curves (solid line) the observed values ΔF_{ob} for flight *F 3* as an example are shown (dashed line) together with a curve ΔH_u calculated from Untiedt’s (1967) model without reversed currents. The observational results are in good agreement with

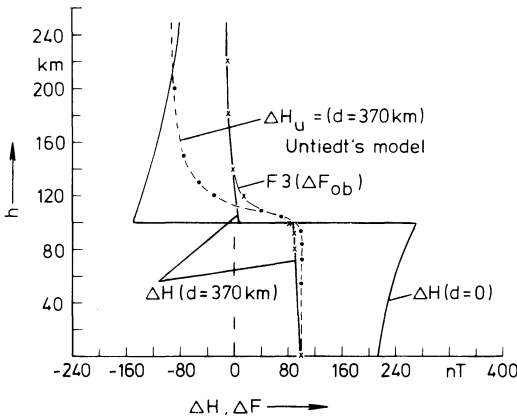


Fig. 11. Model calculations of the ΔH variation with height for $d = 370$ km (Natal) and $d = 0$ (Fortaleza) including reversed currents. $d =$ distance from the magnetic equator. The observed ΔF_{ob} variation for flight F3 is added to show how well the calculations and the observations agree. Also included is the field variation $\Delta H_U(h)$ for $d = 370$ km as calculated by Rippen (1975) according to Untiedt's (1967) model

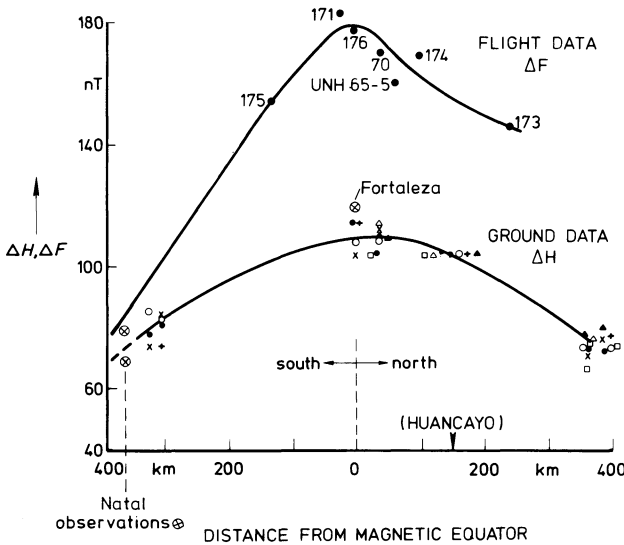


Fig. 12. Ground observations of ΔH and flight observations of ΔF in Peru for various distances from the magnetic equator as presented by Davis et al. (1967). Included are the measurements of ΔH on ground in Natal and Fortaleza (normalized to the scale selected by Davis et al.) as well as the flight data of ΔF above Natal

the simple model calculations also for the other flights, so that the introduction of reversed currents also removes the first discrepancy.

Using this model it is also possible to explain the rocket flight results of Davis et al. (1967) in more detail. At Natal a ratio of 1:1 for $\Delta H : \Delta F_{ob}$ was observed for all flights under regular magnetic conditions (see Table 1). But as can be seen from Figure 11 this ratio is a function of the distance d from the magnetic equator, reaching a value of 1:2 for $d = 0$ km. This is in agreement with observations of Davis et al. (1967) who measured ΔF (flight) and ΔH (ground) as a function of latitude. For comparison their results are shown in Figure 12 together with our results. Thus it seems that with the model described above not only the amount of the ΔF variation but also its latitudinal dependence as observed by Davis et al. (1967) can be explained.

Conclusions

It was the aim of the rocket experiments to verify the existence of meridional currents in the equatorial ionosphere. The results obtained clearly indicate such currents, but the measured values of ΔF and ΔD_M (in Tables 1 and 2) can be explained only by taking into account reversed currents. The strengths of these reversed currents giving the best fit to the observed results were calculated. Similar values were deduced from ground-based measurements. With the assumption of reversed currents the observed variation of ΔF with latitude can also be explained. Although not all details of the observations can be explained by this simple model, some understanding of the observed ΔF and ΔD_M variations seems possible. However, up to now there are no simultaneous measurements in the ionosphere of the electrojet and its reversed currents. To get a better picture of the electrojet phenomena simultaneous rocket measurements at at least three different distances from the magnetic equator should be carried out: At the equator to get the maximum effect of the electrojet, at the center of the reversed currents which is at about 500 km north respectively south of the magnetic equator, and at about half this distance. In addition to the rocket borne measurements ground based observations of the earth's magnetic field on a profile perpendicular to the magnetic equator should be carried out also. The influence of the Sq-currents can only be calculated if there are observations at a distance far enough from the magnetic equator. Therefore ground stations at 3,000 to 4,000 km off the equator should be included. With actual values of magnetic variations along a groundbased profile of some thousand kilometers and ionospheric observations at three different distances one should be able to distinguish between the different current systems. Besides some minor changes the payload described here seems to be suitable for ionospheric measurements, and especially for the observation of meridional currents.

Acknowledgements. We are grateful to Professor Dr. W. Kertz, Director of the Institut für Geophysik und Meteorologie der Technischen Universität Carolo-Wilhelmina, Braunschweig, for his support, advice and the computations of model current systems. Thanks are also due to Mr. D. Hesse, also Braunschweig, and Professor J. Untiedt, Münster, for valuable discussions.

This work was supported financially by the Bundesministerium für Forschung und Technologie.

References

- Aikin, A.C., Blumle, L.I.: Rocket measurements of the E-region electron concentration in the vicinity of the geomagnetic equator, *J. Geophys. Res.* **73**, 1619–1626, 1968
- Cain, J.C., Hendriks, W.E., Jensen, D.C.: Computation of the main geomagnetic field from spherical harmonic expansions. Data Users Note NSSDC 68–11. National Space Science Data Center, Greenbelt, 1968
- Davis, T.N., Burrows, K., Stolarik, J.D.: A latitude survey of the equatorial electrojet with rocket-borne magnetometers. *J. Geophys. Res.* **72**, 1845–1861, 1967
- Fambitakoye, O., Mayaud, P.N.: Equatorial electrojet and regular daily variation S_R . I. A determination of the equatorial electrojet parameters. *J. Atmos. Terr. Phys.*, **38**, 1–17, 1976
- Fambitakoye, O., Mayaud, P.N.: Equatorial electrojet and regular daily variation S_R . II. The center of the equatorial electrojet. *J. Atmos. Terr. Phys.*, **38**, 19–26, 1976

- Fambitakoye, O., Mayaud, P.N., Richmond, A.D.: Equatorial electrojet and regular daily variation S_R . III. Comparison of observations with a physical model. *J. Atmos. Terr. Phys.*, **38**, 113–121, 1976
- Jacobs, K.G., Rawer, K.: Electron density measurements in the ionosphere over the sahara with a variable frequency impedance probe, *Space Res.* **5**, 706–718, 1965
- Jacobs, K.G., Rawer, K.: Raketenmessungen mit einer Hochfrequenz-Impedanzsonde, *Jahrbuch 1966 der WGLR*, 378–384, 1966
- Maynard, N.C.: Measurements of ionospheric currents off the coast of Peru, *J. Geophys. Res.*, **72**, 1863–1875, 1967
- Melzner, F., Rabben, H.H.: Elektronendichte-Messungen in der Ionosphäre mit einer neuartigen HF-Impedanzsonde. *Z. Geophys.* **36**, 135–150, 1970
- Mühlhausen, K.H.: Elektronendichtemessungen in der Ionosphäre, Auswertung des Impedanzsondenexperiments der EEJ-Raketen. Diplom-Arbeit, Institut für Geophysik und Meteorologie der Technischen Universität Braunschweig, Braunschweig, 1974
- Musmann, G.: Verfahren zur Lagemessung von Raketen. *GAMMA 15*, Institut für Geophysik und Meteorologie der Technischen Universität Braunschweig, Braunschweig, 1971
- Musmann, G., Seiler, E., Hansel, J.: Bodenmessungen während der EEJ-Raketenkampagne in Brasilien, Oktober 1970. *GAMMA 19*, Institut für Geophysik und Meteorologie der Technischen Universität Braunschweig, Braunschweig, 1971
- Richmond, A.D.: Equatorial electrojet. I. Development of a model including winds and instabilities. *J. Atmos. Terr. Phys.*, **35**, 1083–1103, 1973
- Rippen, H.: Anwendung eines meridionale Ströme berücksichtigenden Modells auf den äquatorialen Elektrojet in Brasilien. Diplom-Arbeit, Institut für Geophysik und Meteorologie der Technischen Universität Braunschweig, Braunschweig, 1975
- Sastry, T.S.G.: Daily Variation of Geomagnetic Field at the Indian Stations under the Electrojet during Period of the July 1966 Proton Flare. *J. Geophys. Res.*, **78**, 1692–1698, 1973
- Sugiura, M., Poros, D.J.: An improved model equatorial electrojet with a meridional current system. *J. Geophys. Res.*, **74**, 4025–4034, 1969
- Untiedt, J.: A model of the equatorial electrojet involving meridional currents. *J. Geophys. Res.*, **72**, 5799–5810, 1967

Received June 24, 1977; Revised Version December 23, 1977